

Primordial galactic magnetic fields: An application of QCD domain walls.

Michael McNeil Forbes and Ariel R. Zhitnitsky

*Department of Physics and Astronomy, University of British Columbia
Vancouver, British Columbia, Canada, V6T 1Z1.*

We present a mechanism for generating primordial magnetic fields with large correlation lengths on the order of 100 kpc today. The mechanism is based on recently conjectured QCD domain walls or similar CP violating domain walls with QCD scale structure. Such domain walls align the electric and magnetic dipole moments of the nucleons shortly after the QCD phase transition, producing electromagnetic fields correlated along the domain walls. Through the Kibble mechanism, the domain walls attain Hubble-scale correlations which they transfer to the aligned electromagnetic fields. Due to the CP violation, the Hubble-scale walls produce helical (non-zero Chern-Simons) magnetohydrodynamic turbulence which then undergoes an inverse cascade, allowing the correlation lengths to grow to 100 kpc today. We present an estimate the magnitude of the generated electromagnetic fields in terms of the QCD parameters. We also discuss some other unexplained astrophysical phenomena which may be related to this mechanism. In particular, we discuss the relation between primordial magnetic fields and the Greisen-Zatsepin-Kuzmin (GZK) cutoff violations. We also outline how, by creating inhomogeneities in the nucleon density, QCD domain walls may lead to inhomogeneous big bang nucleosynthesis (IBBN) explaining the Ω_B excess recently measured through cosmic microwave background (CMB) distortions.

PACS numbers: 98.62.En, 14.80.Mz, 12.38.Lg

I. INTRODUCTION

The purpose of this paper is to present a careful argument of the mechanism outlined in our letter [1] to generate large scale cosmic magnetic fields. It is an extended and updated version of the letter [1] and the conference proceedings [2] and should be considered to be the definitive version of these papers.

Many different observations suggest that there exist substantial (microgauss) magnetic fields in the universe today [3, 4], however, there has yet to emerge a theory which adequately explains the origins of these fields. Most of the data on large scale astrophysical magnetic fields comes from the observation of synchrotron radiation emitted in galaxies. This radiation is plane polarized, and as it passes through magnetic fields, the plane of polarization rotates due to the Faraday effect: an effect which depends on the frequency of the radiation and the strength and orientation of the magnetic fields. By comparing several sources or radiation with different frequencies, one can extrapolate to determine the original plane of polarization and then estimate the magnetic field strengths.

What is striking, is not just the existence of magnetic fields, but that they appear to be microgauss fields which have correlations as large as 500 kpc in clusters. To put this into perspective, the luminous core of galaxies have typical scales of up to 10 kpc while it is estimated that the galactic dark matter halos extend to 50 kpc. Thus, it seems that galactic dynamo mechanisms cannot produce these large correlation lengths.

The current models for producing these fields involve two main processes: 1) dynamical amplification and/or generation of magnetic fields by galactic processes (galactic mechanisms) and 2) primordial mechanisms which

take place prior to gravitational structure formation. The galactic mechanisms are primarily based on gravitational dynamos, although there are suggestions that supernovae or other stellar phenomena may play a role. While it is likely that galactic dynamos amplify fields, it seems difficult to account for the large scale correlations of the magnetic fields when only galactic mechanisms are considered. It is also not certain that galactic mechanisms can generate magnetic fields: instead they serve only as an amplifier requiring seed fields to be present for the dynamo to work.

The inadequacies of the galactic mechanisms have led to many proposals that the magnetic fields may have a primordial origin. In this case, some process in the early universe (typically at a cosmic phase transition or during inflation) is thought to generate magnetic turbulence. This turbulence then sustains itself as the universe expands and what we observe are the remnants of this turbulence. Most primordial sources, however, also produce fields which end up with very small correlations today or which are very weak.

Most likely, a complete picture of the history of astrophysical magnetic fields requires some primordial inputs as well as amplification through gravitational dynamics. In this paper, however, we discuss a primordial mechanism which seems to naturally produce fields of 100 kpc correlations today. In combination with dynamic amplification mechanisms, we hope that this mechanism might provide a solid foundation for the theory of large-scale astrophysical magnetic fields.

At this point we would like to refer the reader to the several reviews and sample papers in this field. The primary discussions of observations, which contain reviews of the theory, are presented in [3, 4]. Good current reviews are given in [5, 6, 7]. Many different types of

primordial mechanisms are discussed, for example: Inflationary mechanisms [8], cosmic strings [9, 10], charge asymmetries [11, 12], and phase transitions [13, 14]. The evolution of primordial magnetic fields is discussed in [7, 15, 16]. In particular, the inverse cascades discussed here will be important for our mechanism.

II. OVERVIEW OF THE MECHANISM

The mechanism that we propose has the following core components:

1. Sometime near the QCD phase transition, $T_{\text{QCD}} \approx 1$ GeV, domain walls form which can interact with QCD scale physics.
2. These domain walls rapidly coalesce until there remains, on average, one domain wall per Hubble volume with Hubble scale correlations.
3. Baryons interact with the domain walls and align their spins along the walls. The Hubble scale correlation of the domain walls thus induces a Hubble scale correlation in the spin density.
4. The anomalous magnetic and induced electric dipole moments of the baryons generate helical electromagnetic fields also correlated on the Hubble scale.
5. The domain walls move rapidly and vibrate, effectively filling the Hubble volume with helical magnetic turbulence with a Hubble scale correlation.
6. The domain walls decay and the electric fields are screened leaving magnetic turbulence with Hubble scale correlations.
7. As the universe expands, an “inverse cascade” mechanism transfers energy from small to large scale modes, effectively increasing the resulting correlation lengths but diluting the field strengths.
8. Galactic dynamos amplify the fields in galaxies, but the fields should also persist in the extra-galactic media.

The idea that domain walls might generate magnetic fields is not original. For example, it was suggested that standard axion domain walls could be ferromagnetic in [17], however mechanism discussed there seems to be flawed: The scale of the standard axion walls is of the order m_a^{-1} which is at least some twelve orders of magnitude larger than the QCD scale $\Lambda_{\text{QCD}}^{-1}$ (m_a is the axion mass). It is hard to see how these walls can efficiently affect QCD physics at the temperatures that were present

in the early universe where thermal fluctuations will destroy all coherence.¹

Another problem with proposals including standard axion domain walls is that these walls must decay to prevent cosmological problems [19]. There are still questions about how the standard so-called $N \neq 1$ axion domain walls can decay.

In this paper, we outline the properties that domain walls must have to generate sufficient magnetic seed fields. The exact source could be one of several types of walls, including modified axion domain walls, or entirely different types of walls. To be concrete, we present our model in terms of a recently conjectured quasi-stable QCD domain wall [20] which may exist, either independently of axion physics, or along with a dynamical axion adding additional QCD scale structure to the standard axion domain walls. These domain walls are characterized by a transition in the singlet η' field which has a size and energy scale set by Λ_{QCD} . Hence, QCD domain walls can directly couple to QCD physics. In addition, the singlet field transition at the center of the wall induces an effective non-zero CP violating θ background which in turn will induce an electric dipole moment and alter the magnetic dipole moment in the fermions [21] so that both the electric and magnetic dipole moments of all the particles are on the same order. In the presence of these anomalous dipole moments, the cancellations discussed in [22, 23] in the domain wall background are no longer a problem.

Another crucial aspect of our mechanism is the “inverse cascade” which governs the evolution of the magnetic fields after they are formed. This mechanism was suggested by Cornwall [24], discussed by Son [25] and confirmed by Field and Carroll [26]. It is based on the idea that magnetic helicity (Abelian Chern-Simons number) $H = \int \vec{\mathbf{A}} \cdot \vec{\mathbf{B}} d^3x$ is approximately conserved in the universe where temperatures are higher than $T_0 \approx 100$ eV. This conservation of helicity causes energy to cascade up the turbulent modes increasing the energy in large scale modes and increasing the effective correlation length of the turbulence. The importance of helicity was originally demonstrated by Pouquet and collaborators [27]. Without this helical inverse cascade, there is no known way to generate large correlations fields today from sub-Hubble scale fields in the early phase transition and one must consider super-Hubble scale correlations resulting from inflationary schemes. It turns out, however, that Hubble scale correlations at the QCD phase transition (the last major phase transition) provide correlations on the order of 100 kpc today: thus it is natural to consider QCD physics as the source of primordial

¹ For some other discussions about the magnetic properties of the domain walls, see [18] and reference therein. We should note, however, that in all these discussions, the most difficult problem of generating large scale correlations has not been addressed.

fields (earlier physics can only produce even smaller correlations).

Perhaps the least understood aspect of this mechanism concerns the dynamics of the domain walls and the interactions of the domain walls, nucleons and electric and magnetic fields. As we shall show, all of these components interact on the same scale of Λ_{QCD} and hence there are complication back-reactions and nonlinear dynamics. We presently do not have the tools to fully analyze these features, but we present here in detail quantitative estimates and calculations which we believe are good estimates of the scale of the effects.

The result is a mechanism which naturally produces magnetic fields today with $l \sim 100$ kpc correlations and with strengths of

$$B_{\text{rms}} \sim \frac{10^{-9}\text{G}}{\xi\Lambda_{\text{QCD}}}, \quad l \sim 100 \text{ kpc} \quad (1)$$

where the parameter $1 \leq \xi\Lambda_{\text{QCD}} \ll 10^{19}$ depends on the dynamics of the domain walls as discussed in section (IV). If the correlation ξ turns out to be small, then this mechanism might generate detectable extra-galactic fields, otherwise we still require a galactic dynamo to amplify the fields. In any case, however, these seeds still maintain the large scale correlations of the observed fields, and it seems that even if ξ is large, the resulting fields may be strong enough to seed the galactic dynamos [28].

We shall begin by discussing the inverse cascade mechanism in section (III) and then give estimates of the field strengths in an idealized case of static, flat walls. Finally, we shall discuss the dynamics of the domain walls and describe the whole process, justifying the mechanism.

III. EVOLUTION OF MAGNETIC FIELDS

Given a stable magnetic field configuration in the universe, one might naïvely expect the size of the correlations of the field to expand with space as governed by the universe's scale parameter $l \propto R(T)$ and the field strength to be correspondingly diluted $B \propto R(T)^{-2}$. It was discovered by Pouquet and collaborators [27], however, that if the magnetic fields have a non-zero helicity (Abelian Chern-Simons number) $H = \int \vec{\mathbf{A}} \cdot \vec{\mathbf{B}} d^3x$, then the fields will scale differently. Cornwall [24] suggested that helical fields might undergo an inverse cascade. The magnetohydrodynamic (MHD) equations were subsequently studied by Son [25] who derived the scaling relations (2) presented below. These have subsequently been confirmed by Field and Carroll [26].

The reason for the scaling is that the magnetic helicity H is an approximately conserved quantity in the early universe. It is also known that the small scale turbulent modes decay more rapidly than the higher scale modes. In order to conserve the helicity as the small scale modes decay, the helicity must be transferred to larger modes

and with this transfer of helicity is a transfer of energy. This is the source of the inverse cascade.

To understand the origins of the conservation of helicity, note that it is a topological quantity that describes the Gaussian linking number of the vector potential lines of flux (see for example [29]). In a perfectly conducting medium, these lines of flux cannot cross, and hence there is no way to unlink the flux lines: helicity is perfectly conserved. Even when the conductivity is finite, the helicity is also well conserved.

There is a direct analogy with fluid mechanics. The equivalent there is vorticity $\zeta = \int \vec{\mathbf{v}} \cdot (\vec{\nabla} \times \vec{\mathbf{v}}) d^3x$ which is the Gaussian linking number of the fluid flow lines. If the fluid has no viscosity, then ζ is perfectly conserved. Even viscous fluids, however, approximately conserve vorticity. This is why, for example, smoke rings and tornados are so stable.

We shall not derive the scaling relationships here, instead we refer the reader to [25, 26], however, we summarize here the results:

$$B_{\text{rms}}(T_{\text{now}}) = \left(\frac{T_0}{T_{\text{now}}}\right)^{-2} \left(\frac{T_i}{T_0}\right)^{-7/3} B_{\text{rms}}(T_i) \quad (2a)$$

$$l(T_{\text{now}}) = \left(\frac{T_0}{T_{\text{now}}}\right) \left(\frac{T_i}{T_0}\right)^{5/3} l(T_i). \quad (2b)$$

These relate the initial field strength $B_{\text{rms}}(T_i)$ with initial correlation $l(T_i)$ to the present fields today ($T_{\text{now}} \approx 2 \times 10^{-4}$ eV) $B_{\text{rms}}(T_{\text{now}})$ with correlation $l(T_{\text{now}})$. During the period when the universe supports turbulence (as indicated by a large Reynolds number Re), the inverse cascade mechanism functions and have the scalings $B \propto T^{7/3}$ and $l \propto T^{-5/3}$ as indicated by the second factors in (2). In the early universe, Re is very large and the turbulence is well supported. As the universe cools, eventually, for temperatures below some T_0 , the turbulence is no longer well supported. Exactly what the effective temperature T_0 the turbulence ceases is not clear: Son points out that at $T_0 \approx 100$ eV, the Reynolds number drops to unity and thus turbulence is not well supported because of the viscosity of the plasma [25]. We take this as a conservative estimate. Field and Carroll argue that the turbulence is force-free and so unaffected by the viscosity. Thus they take $T_0 \sim 1$ eV at the epoch when the matter and radiation energy densities are in equilibrium and argue that the cascade may even continue into the matter dominated phase of the universe. If this is true, then it might be possible to increase the correlation lengths of the fields by one or two orders of magnitude from the conservative estimate (1). In any case, for temperatures lower than T_0 , the turbulence and inverse cascade are not supported and so we assume that the fields are ‘‘frozen in’’ and experience only the naïve scaling $l \propto T^{-1}$ and $B \propto T^2$ indicated by the first factors in (2).

As pointed out by Son [25], the only way to generate turbulence is either through a phase transition T_i or through gravitational instabilities. Thus, until gravitational dynamos are active, the scalings (2) should be

valid. In any case, galactic dynamos will amplify the fields, but will not affect the correlation length, so in particular, (2b) should be a good estimate, regardless of galactic dynamics (the uncertainty come during the transition period $T \sim T_0$ when the scaling laws change. The estimate (2b) is generally considered conservative in this sense as the cascade likely continues for some time past T_0 [26].

Now we consider the source of the magnetic turbulence at a phase transition. As we shall show, our mechanism generates Hubble size correlations l_i at a phase transition T_i . In the radiation dominated epoch, the Hubble size scales as T_i^{-2} . Combining this with (2b), we see that $l_{\text{now}} \propto T_i^{-1/3}$; thus, the earlier the phase transition, the smaller the resultant correlations.

The last phase transition is the QCD transition, $T_i = T_{\text{QCD}} \approx 0.2$ GeV with Hubble size $l(T_{\text{QCD}}) \approx 30$ km. With our estimates (46) of the initial magnetic field strength $B_{\text{rms}}(T_i) \approx e\Lambda_{\text{QCD}}^2/(\xi\Lambda_{\text{QCD}}) \approx (10^{17}\text{G})/(\xi\Lambda_{\text{QCD}})$ we use Equations (2) to arrive at the estimate (1). The meaning of the correlation length ξ will be discussed in detail later in section (VII). The most important result here is that, as long as one has a mechanism to generate Hubble scale correlations and a maximally helical magnetic field at the QCD phase transition, magnetic turbulence of 100 kpc correlations is naturally produced. The questions: ‘How can helical magnetic fields with Hubble-scale correlations be produced at the QCD phase transition’ and, ‘Are these fields strong enough to account for the observed microgauss fields?’ will be addressed in the rest of this paper. The estimate (1) suggests, however, that even in the worst case of almost maximal suppression $\xi\Lambda_{\text{QCD}} \sim 10^{19}$, an efficient galaxy dynamo may be able to amplify the fields to the microgauss level. In the best case, the mechanism would produce measurable extra-galactic fields.

In either case, the important result is the generation of the 100 kpc correlations: if observations show that the fields have much larger correlations, then the proposed mechanism can only be salvaged if a more efficient ‘inverse cascade’ mechanism is shown to work between T_{QCD} and now. Having said this, one might consider the electroweak or earlier phase transitions. As we mentioned, the earlier the phase transition, the smaller the resulting correlations $l_{\text{now}} \propto T_i^{-1/3}$. For the electroweak transition, the scaling (2b) suggests that Hubble scale helical fields could generate 100 pc correlations today. Thus it might be possible that electroweak phenomena could act as the primordial source, but this presupposes a mechanism for generating fields with Hubble scale correlations. Such a mechanism does not appear to be possible in the Standard Model. Instead, the fields produced are correlated at the scale T_i^{-1} which can produce only ~ 1 km correlations today which are of little interest.

Thus, the previous analysis seems to suggest that, in order to obtain magnetic fields with 100 kpc correlation lengths, helical fields must be generated with Hubble scale correlations near or slightly after the QCD phase

transition T_{QCD} . The same conclusion regarding the relevance of the QCD scale for this problem was also reached by Son, Field and Carroll [25, 26]. Without further ado, we now present our picture of the mechanism and justify the estimate (1) of the magnetic field strength.

IV. GENERATION OF MAGNETIC FIELDS BY DOMAIN WALLS

The key players in this mechanism are domain walls which form shortly after the QCD phase transition. Details of the walls were presented in [20] which will be summarized in section (V). In sections (VI) and (VII) we shall show that these walls tend to align nuclear magnetic and electric dipole moments along the plane of the wall. An important feature of the walls is that across the wall there is maximal strong CP violation due to an induced nonzero θ . Because of this, the electric and magnetic dipole moments of the nucleons are of the same order. Thus, both neutrons and protons will have nonzero electric and magnetic dipole moments and play a role in generating the electromagnetic fields.

Because of the correlation between the electric and magnetic fields along the domain wall, the generated fields have an induced helicity as we shall examine in section (VII). This helicity has the same sign along the entire domain wall and we expect that the domain wall will fill the entire Hubble volume, thus the helicity will be correlated on the Hubble scale.

Finally, the domain walls will decay as discussed in [20] so that the universe is not dominated by domain walls today. By this point, however, the helical magnetic turbulence has been generated.

A. Hubble Size Correlations

The reason that we feel domain walls hold the key to explaining primordial magnetic seeds is that in a short time they can generate Hubble scale correlations. The initial fields must have a Hubble scale correlation or else there is no known way—even with the inverse cascade—to generate the huge correlations today. Let us briefly summarize what we expect to be the behaviour of domain walls at the QCD phase transition. For a nice description of general domain wall dynamics see [19] from which most of these results were derived.

1. Prior to the phase transition $T_i = \Lambda_{\text{QCD}}$, the fields are in random fluctuations on the scale T_i and domain walls are not present.
2. After the phase transition, however, the fields settle into their vacuum states. Domains are formed

where the fields are settling into different² vacuum states. These domains are separated by domain walls and have a scale set by Λ_{QCD} .

3. Numerical studies suggest that these small-scale domain walls rapidly merge increasing the correlation length of the walls. This coarsening occurs simultaneously throughout space and the correlation length of the domain walls can increase faster than the speed of light.
4. The coarsening stops once the domain walls attain a Hubble scale. On average, one ends up with one domain wall per Hubble volume, but which curls and moves through space, essentially filling the volume.

It is these Hubble sized domain walls that can generate magnetic turbulence with Hubble size correlations. As we shall see below, there are two types of domain walls corresponding to opposite field transitions. One we call a “soliton”, and the other we call an “anti-soliton”. Together a soliton and an anti-soliton can annihilate, but the coarsening essentially separates regions of solitons from anti-soliton regions by a distance of the Hubble scale so that they do not annihilate. In section (VII A) we shall show that the solitons and anti-solitons are associated with helicity of the opposite sign. Thus, the domain walls effectively separate the helicity generating a Hubble scale correlation length in the fields and in the helicity.³

² In the case of QCD domain walls, the vacuum states are actually the same but the field configuration going from one domain to the next undergoes a classically stable transition. This behaviour is qualitatively similar to the sine-Gordon model $\mathcal{L}_{\text{SG}} = (\partial_\mu \phi)^2 - \cos \phi$ where ϕ is interpreted as a phase so that the vacuum states $\phi = 2\pi n$ are actually identical.

³ There is some question about what conditions must be like at the phase transition in order for domain walls to form. QCD lattice simulations suggest that at low densities (such as those present in the early universe), the transition between the quark-gluon plasma and the normal hadronic phase is a smooth crossover and that the critical point sits at some finite density (see the recent review [30]). If the rate at which the universe cools is sufficiently slow, then it is possible that no domain walls will form. In the preface to the paperback edition [19], the authors discuss this scenario as the Kibble-Zurek picture: to estimate the size of the correlations produced, one must consider the relaxation timescale $\tau(T)$ that it takes to establish correlations on the scale $\xi(\tau)$. The freezeout temperature T_f is determined by the condition $\tau \sim t_D = |T - T_c|/|\dot{T}|$, i.e. when the relaxation time is on the same order as the dynamical timescale of temperature variations. Since the true critical point is at a somewhat higher densities than the universe, t_D may be bounded from below and if the cooling is sufficiently slow, it is possible that $\tau \ll t_D$ and domain walls will not form. To estimate these effects requires a better understanding of the dynamics of the domain walls and of the phase transition than we presently have. We assume that the dynamics are such that domain walls do form and coalesce forming Hubble-scale correlations as described in [19].

B. Essential Domain Wall Properties

Thus, we can formulate a set of properties that must be satisfied by domain walls if they are to be considered as sources for the primordial magnetic fields described in this paper:

1. The walls must attain Hubble scale correlations near the QCD phase transition to generate the observed correlations.
2. The walls must have structure on the scale of Λ_{QCD} in order to interact effectively with nucleons.
3. There must be some way to avoid the cancellations discussed in [22, 23] so that the walls are ferromagnetic rather than diamagnetic.
4. The walls must somehow induce a definite helicity throughout the Hubble volume.
5. The domain walls must be unstable or have other features so that the problems of domain wall domination in the universe are avoided, but they must be stable enough that they can generate the appropriate fields. They must also leave nucleosynthesis production ratios relatively unaffected.

It seems to be a rather general property of cosmological domain wall networks that they rapidly coarsen through the Kibble mechanism until the walls have a Hubble-scale correlation length [19]. Thus, criterion 1 should be easily satisfied by almost all types of domain walls. Criterion 2 rules out the standard axion domain walls discussed in [17, 31, 32], however, there may be features of these walls that have QCD scale which were previously neglected. In particular, Shifman and Gabadadze discuss a gluonic core sandwiched at the center of axion domain walls [33] which they call D-walls. This structure has a QCD scale and may be able to align nuclear matter.

In our paper [20] we discuss another possibility: that the η' field may provide domain wall structure with QCD scale. This structure, which we shall refer to as a QCD domain wall, can exist within the standard axion domain wall providing the required QCD scale structure, but can also exist, even if there is no axion (unlike the D-walls of [33] which require an axion field).

A further property of QCD domain walls and axion domain walls is that, at their center, there is strong CP violation. This CP violation has several effects as described in section (IV C). In particular, the CP violation induces an anomalous electric dipole moments in nucleons. Thus, CP violating domain walls can satisfy criterion 3.

Helicity is also associated with CP violation as it is a CP odd quantity. As discussed above, the soliton and anti-soliton domain walls solutions have opposite CP. Thus, each is associated with opposite helicity. Typically, the solitons and anti-solitons separate spatially so that Hubble-sized regions are filled with one type or another. The helicity is generated through the correlation

of both electric and magnetic fields along the walls. Thus, the Hubble scale spatial separation of soliton and anti-soliton domain walls also separates the helicity and thus generates helical turbulence with Hubble scale correlations satisfying criterion 4.

Another major problem with axion domain walls is that most varieties appear to be absolutely stable. The $N = 1$ axion model discussed recently by Chang, Haggmann and Sikivie [32] has a decay mode that satisfies the criterion 5. However, this is not a phenomenologically acceptable model and, to date, the other axion models are plagued by this problem. If axion domain walls are to be considered, then a satisfactory solution to this problem must be found.

The QCD domain walls [20] without an axion, exhibits a similar decay mode to the the $N = 1$ axion model. The scales, however, are set by Λ_{QCD} rather than m_a and so criterion 5 must be address from the point of view: Do the walls live long enough to generate the turbulence? As addressed in [20], the answer may be yes. The only decay mode is through a nucleation process suppressed by quantum mechanical tunneling. Consequently, these walls may have a macroscopic lifetime long enough to generate the fields. In any case, however, they decay fast enough to avoid affecting nucleosynthesis and other cosmological effects.

Thus, there may be several types of domain walls that could act as sources for primordial magnetic seed fields. In this paper, we now specialize to discuss the QCD domain walls presented in [20] showing that they may be able to generate sufficiently large magnetic fields to seed galactic dynamos and possibly observe in the extragalactic medium.

C. Strong CP Violations in Domain Walls

We present a brief summary here of the essence of strong CP violation to explain how axion and QCD domain walls may satisfy the criteria discussed above. The most general form for the fundamental QCD Lagrangian is known to contain the following term related to the anomaly:

$$\mathcal{L}_\theta = \frac{\theta g^2}{32\pi^2} G_{\mu\nu}^a \tilde{G}^{a\mu\nu} \quad (3)$$

where $G_{\mu\nu}^a$ is the gluon field tensor and $\tilde{G}^{a\mu\nu} = \frac{1}{2}\varepsilon^{\mu\nu\rho\sigma} G_{\rho\sigma}^a$ is its dual. This term is odd under the discrete symmetry CP, thus, if θ is non-zero, then the strong interaction should violate CP. Experiments, however, have placed tight limits $|\theta| < 10^{-9}$. The contributions to the final θ arise from several sources, and it remarkable that these seem to exactly cancel. The origin of this cancellation is known as the strong CP problem.

One solution is to promote θ from a parameter to a dynamical field called the axion [34, 35]. The idea is that, prior to the QCD phase transition, the axion field is massless and θ can take on any value. After the transition, the

axion acquires a mass and sits in a potential with a minimum energy where $\theta = 0$. The axion field thus relaxes to the minimum restoring CP conservation today. To date, axions have not been detected, however, there is an allowed region consistent with experimental, astrophysical and cosmological constraints: Thus, the so-called invisible axion [36, 37], which is very light: $m_a \sim 10^{-5}$ – 10^{-3} eV, may still resolve the strong CP problem. In addition, axions of this mass are very strong cold dark candidates (see for example the recent review [38]). As mentioned, axions provided a nice mechanism for generating domain walls, but because the axion must be so light, there is no way for such structures to efficiently interact with nucleons. For a good reviews of the strong CP problem and the role of axions, see [39, 40, 41].

In any case, we assume that some method exists to solve the strong CP problem. What is important about the θ parameter is that, in the low-energy limit, it only appears in the combinations $(\theta + \phi)$ (Equation 9) and $(\theta + \phi - a)$, where ϕ is the dynamical field related to the η' meson and a is the axion field. Thus, even when $\theta = 0$, CP will be violated in strong interactions in a domain wall background where ϕ or $\phi - a$ is non-zero over a macroscopically large region. Hence, QCD and axion domain walls induce strong CP violations over their central regions.

One of the consequences of this strong CP violation is that nucleons have an induced electric dipole moment as well as a magnetic dipole moment⁴ [21]. We summarize those results here.

In the chiral limit $m_q \rightarrow 0$ for small θ

$$d_N \simeq \frac{e g_{\pi NN} \bar{g}_{\pi NN}}{4\pi^2 m_N} \ln\left(\frac{m_N}{m_\pi}\right), \quad (4)$$

where $g_{\pi NN}$ is the strong πNN coupling constant and $\bar{g}_{\pi NN}$ is the CP odd πNN coupling constant which was estimated to be $\bar{g}_{\pi NN} \sim 0.04|\theta|$. In these formulae the θ parameter should be treated as the singlet ϕ domain wall solution $\phi(z)$ with nontrivial z dependence. From these formulae one can compute the following relation

$$\frac{d_\Psi}{\mu_\Psi} \sim \frac{g_{\pi NN} m_q}{2\pi^2 f_\pi} \ln\left(\frac{m_N}{m_\pi}\right) \theta(z) \simeq 0.1. \quad (5)$$

Thus, for all nucleons, including the neutron, both the electric and magnetic dipole moments are non-zero and of the same order in the domain wall background when $\theta(z) \equiv \phi(z) \sim 1$.

V. QCD DOMAIN WALLS

We saw in section (IV B) that several types of domain walls might act as sources for seed fields. To be concrete,

⁴ Normally the electric dipole moment is suppressed to the same order as θ in that CP is conserved.

we shall now restrict our attention to QCD domain walls to show how domain walls might produce magnetic seed fields. In this section, we shall present a short review of the results presented in [20], simplifying the model for presentation.

To describe these walls, we consider the low-energy effective theory of QCD including the pions and the η' singlet field. The η' field is not as light but is the source of the physics behind the QCD domain walls. The pions and η' enter the Lagrangian through the matrix representation

$$\mathbf{U} = \exp \left[i\sqrt{2} \frac{\pi^a \lambda^a}{f_\pi} + i \frac{2}{\sqrt{N_f}} \frac{\eta'}{f_{\eta'}} \right] \quad (6)$$

where π^a are the $N_f^2 - 1$ pseudo-Goldstone fields, λ^a are the Gell-Mann matrices for $SU(N_f)$ and η' is the singlet field. From now on, we limit ourselves to the simplest case of one flavour $N_f = 1$ which contains only the η' field but captures all the relevant physics. The $N_f = 2$ case is presented in [20]. Although the models are quantitatively different, the phenomena described by both is the same. In this model, we see that (6) reduces to a single complex phase

$$\mathbf{U} = e^{i\phi}, \quad \phi = \frac{2\eta'}{f_{\eta'}}. \quad (7)$$

The effective Lagrangian density then reduces to

$$\mathcal{L} = \frac{f_{\eta'}^2}{8} (\partial_\mu \phi)^2 - V(\phi) \quad (8)$$

with the effective potential

$$V(\phi) = - \min_l \left\{ M \cos \phi + E \cos \left(\frac{\theta + \phi + 2\pi l}{N_c} \right) \right\} \quad (9)$$

which was first introduced in [42]. The minimization on the right comes from choosing the lowest energy branch of the multi-valued potential. Details about this potential are discussed in the original paper [42] but several points will be made here. All dimensionful parameters are expressed in terms of the QCD chiral and gluon vacuum condensates: $\mathbf{M} = \text{diag}(m_q^i |\langle \bar{q}^i q^i \rangle|)$ is the mass matrix and $E = \langle b\alpha_s / (32\pi) G^2 \rangle$ is the vacuum energy. These are well known numerically: $m_q \sim 5$ MeV (see for example [43]), $\langle \bar{q}q \rangle \sim -(240 \text{ MeV})^3$ [44], $\langle \alpha_s / \pi G^2 \rangle \sim 0.012 \text{ GeV}^4$ [45] and $b = 11N_c/3 - 2N_f/3$ is the first term in the beta function.

This potential correctly reproduces the Di Vecchia-Veneziano-Witten effective chiral Lagrangian in the large N_c limit [46, 47], it reproduces the anomalous conformal and chiral Ward identities of QCD, and it reproduces the known dependence in θ for small angles [46, 47]. It also exhibits the correct 2π periodicity in θ . This periodicity is the most important property of the potential and is the reason that QCD domain walls form: The qualitative results do not depend on the exact form (cosine) of the

potential. Rather, the domain walls form naturally because of the 2π periodicity ($\theta \rightarrow \theta + 2\pi$) which represents the discrete nature of the ground state symmetries. It is exactly these symmetries which leads to the existence of axion domain walls when θ is promoted to a dynamical axion field [31, 32, 48, 49, 50].

As described in section (IV C), we see that the singlet $U(1)$ field ϕ occurs in the same place as the CP violating θ parameter. Thus, even though to a high degree of precision, $\theta = 0$, in the macroscopic regions where $\langle \eta' \rangle \neq 0$ is non-zero, there will be CP violating physics.

We see that the potential(9) has ground states characterized by

$$\phi_0 = 2\pi n, \quad (10)$$

where n is an integer, with vacuum energy $V_{\min} = -M - E$. Expanding about the minimum $\phi = \phi_0 + \delta\phi$ we find the mass of the field⁵

$$m_{\eta'}^2 = \frac{4}{f_{\eta'}^2} \left(\frac{E}{N_c^2} + M \right) \quad (11)$$

The most important point to realize is that all of the ground states (10) in fact represent the same physical state $\mathbf{U} = \mathbf{1}$. Thus, it is possible for the ϕ field to make a transition $2\pi n \rightarrow 2\pi m$ for different integers n and m . Within this model (8), where all heavy degrees of freedom have been integrated out, these transitions are absolutely stable and represent the domain walls. When one includes the effects of the heavier degrees of freedom, however, we find that the walls are unstable on the quantum level. This is described in detail in [20] and briefly reviewed in the next section.

A. Domain Wall Solutions

To study the structure of the domain wall we look at a simplified model where one half of the universe is in one ground state and the other half is in another. The fields will orient themselves in such a way as to minimize the energy density in space, forming a domain wall between the two regions. In this model, the domain walls are planar and we shall neglect the x and y dimensions: A complete description of this wall is given by specifying the boundary conditions and by specifying how the fields vary along z .

We present here the two basic domain wall solutions. These are characterized by interpolations from the state $\phi = 0$ to:

Soliton: $\phi = 2\pi$,

⁵ In the more general case of N_f quarks with equal masses, the right-hand side of Equation (11) should be multiplied by a factor N_f .

Anti-soliton: $\phi = -2\pi$.

It is possible to consider transitions between further states (i.e. $0 \rightarrow 2\pi n$) but these can be thought of as multiple domain walls. They also have higher energies, are less stable, and are thus less important for our discussion. To gain an understanding of the structure of the domain walls we look for the solution which minimizes the energy density of the domain wall. The energy density (wall tension) per unit area is given by the following expression

$$\sigma = \int_{-\infty}^{\infty} \left(\frac{f_{\eta'}^2}{8} \dot{\phi}^2 + V(\phi) - V_{\min} \right) dz \quad (12)$$

where the first term is the kinetic contribution to the energy and the last term is the potential. Here, a dot signifies differentiation with respect to z : $\dot{a} = \frac{da}{dz}$.

To minimize the wall tension (12), we can use the standard variational principle to arrive at the following equations of motion for the domain wall solutions:

$$\frac{\ddot{\phi} f_{\eta'}^2}{4M} = \sin \phi + \frac{E}{MN_c} \sin \frac{\phi}{N_c}. \quad (13)$$

Again, the last term of Equation (13) should be understood as the lowest branch of a multi-valued function as described by Equation (8).

The general analytical solution of Equations (13) is not enlightening and we present the numerical solution in Fig. 1. In order to gain an intuitive understanding of this wall, we examine the solution in the limit $M \ll E/N_c^2$ (physically, when $N_f > 1$, this is the limit $m_\pi \ll m_{\eta'}$). In this case, the last term of (13) dominates. Thus, the structure of the ϕ field is governed by the differential equation:

$$\ddot{\phi} = \frac{4E}{N_c f_{\eta'}^2} \sin \frac{\phi}{N_c}. \quad (14)$$

Now, there is the issue of the cusp singularity when $\phi = \pi$ because we change from one branch of the potential to another (see Equation (8).) By definition, we keep the lowest energy branch, such that the right-hand side of Equation (14) is understood to be the function $\sin(\phi/N_c)$ for $0 \leq \phi \leq \pi$ and $\sin[(\phi - 2\pi)/N_c]$ for $\pi \leq \phi \leq 2\pi$. However, we notice that the equations of motion are symmetric with respect to the center of the wall (which we take as $z = 0$), hence $\phi = \pi$ only at the center of the wall and not before, so we can simply look at half of the domain, $z \in (-\infty, 0]$, with boundary conditions $\phi(-\infty) = 0$ at $z = -\infty$ and $\phi(0) = \pi$ at $z = 0$. The rest of the solution will be symmetric with $\phi = 2\pi$ at $z = +\infty$.

Equation (14) with the boundary conditions above has the solution

$$\phi(z) = \begin{cases} 4N_c \tan^{-1} \left[e^{\mu z} \tan \frac{\pi}{4N_c} \right], & z \leq 0, \\ 2\pi - 4N_c \tan^{-1} \left[e^{-\mu z} \tan \frac{\pi}{4N_c} \right], & z \geq 0. \end{cases} \quad (15)$$

which is a good approximation of the solution to Equation (13) when $M \ll E/N_c^2$. Here, the scale of the wall is set by the parameter μ :

$$\mu \equiv \frac{2\sqrt{E}}{N_c f_{\eta'}}, \quad \lim_{m_q \rightarrow 0} \mu = m_{\eta'}, \quad (16)$$

which is the inverse width of the wall and which is equal to the field mass $m_{\eta'}$ in the chiral limit $m_q^2 \rightarrow 0$ (see Equation (11)). Thus, we see that, indeed, the QCD domain walls have a QCD scale.

Solution (15) describes the soliton. The anti-soliton can be found by taking $z \rightarrow -z$: thus, we have the transition soliton \rightarrow anti-soliton under the discrete CP symmetry. The numerical solution for the ϕ field is shown in Fig. 1. It turns out that the approximation is reasonable even in the physical case where $N_c^2 M/E \sim 10^{-1}$.

The wall surface tension defined by Equation (12) and can be easily calculated analytically in the chiral limit when the analytical solution is known and is given by Equation (15). Simple calculations leads to the following result:⁶

$$\sigma = 4N_c f_{\eta'} \sqrt{\left\langle \frac{b\alpha_s}{32\pi} G^2 \right\rangle} \left(1 - \cos \frac{\pi}{2N_c} \right) + O(m_q f_{\eta'}^2). \quad (17)$$

In the case when $m_q \neq 0$, σ is numerically close to the estimate (17).

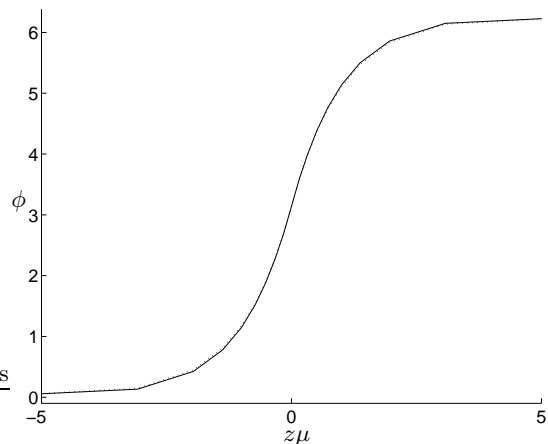


FIG. 1: Basic form of the QCD domain wall (soliton). The analytic approximation (15) is plotted as a dotted line to show the good agreement. We have taken $N_c = 3$ here. Notice that the wall thickness is set by the parameter μ .

⁶ In the general case of N_f quarks of equal mass, the right-hand side of Equation (17) should be multiplied by the factor $1/\sqrt{N_f}$. In this case, it reduces to the result cited in [20] when $N_f = 2$.

B. Domain Wall Decay

Finally, we note that these domain walls are not stable: as mentioned earlier, the vacuum states (10) represent the same physical state. When one includes the heavier gluonic degrees of freedom, it becomes possible for the fields to “unwind” through this extra degree of freedom. Classically this is not allowed because the heavy degrees of freedom are constrained by a large potential barrier, but it is still possible for the field to tunnel through this barrier forming a hole in the domain wall. Once a large enough hole is formed, it will expand and consume the domain wall. This process is called “nucleation” and is similar to the mechanism consuming $N = 1$ axion domain walls [19, 32, 48, 51].

In [20], we estimate the lifetime of these domain walls borrowing the same methods used to estimate the lifetime of axion domain walls in the $N = 1$ axion models [19, 32, 48, 51]. We should point out one major difference, however, between the $N = 1$ axion model and our model. In the axion model, prior to domain wall formation there is a phase where stable axion strings can form. When the domain walls form, these strings bound the domain walls and thus the walls start to decay from the outset greatly reducing their lifetime (see [19] for a nice discussion). In the case of QCD domain walls, strings are not stable objects and do not form before the walls. Thus, the only way for the walls to decay is through the nucleation process we are about to describe. This greatly suppresses the decay rate and is the source of the long lifetime for the walls.

The tunneling probability can be estimated by computing the action S_0 of an instanton solution of the Euclidean (imaginary time, $t = i\tau$) field equations, approaching the unperturbed wall solution at $\tau \rightarrow \pm\infty$. In this case the probability P of creating a hole is proportional to the factor

$$P \sim e^{-S_0} \quad (18)$$

where S_0 is the classical instanton action.

If the radius R_c of the nucleating hole is much greater than the wall thickness, we can use the thin-string and thin-wall approximation. In this case, the action for the string and for the wall are proportional to the corresponding world-sheet areas [51],

$$S_0 = 4\pi R^2 \alpha - \frac{4\pi}{3} R^3 \sigma. \quad (19)$$

Here σ is the wall tension (17), and $\alpha \sim \sqrt{2E}$ is the string tension which we estimate based on dimensional arguments. The string tension α tries to close the hole while the wall tension σ tries to widen the hole. Minimizing (19) with respect to R we find that

$$R_c = \frac{2\alpha}{\sigma}, \quad S_0 = \frac{16\pi\alpha^3}{3\sigma^2}. \quad (20)$$

If a hole forms with radius $R > R_c$ then the hole will expand with time as $x^2 + y^2 = R^2 + t^2$, rapidly approaching the speed of light and consuming the domain wall.

Inserting numerical values for the phenomenological relevant case $N_f = 2$ we find that [20]

$$\alpha \sim (0.28 \text{ GeV})^2, \quad \sigma = (200 \text{ MeV})^3, \quad S_0 \sim 120. \quad (21)$$

What is important is that S_0 is numerically large, and hence the lifetime is much larger than the QCD scale because of the huge tunneling suppression $e^{-S_0} \sim 10^{-52}$. A more complete analysis is presented in [20] where we estimate the lifetime of the walls to be of the order

$$\tau \sim 10^{-5} \text{ s} \quad (22)$$

even though the walls are governed by the microscopic QCD scale. This result should be interpreted with some caution: in the low energy regime, we do not have very good control over the quantitative physics.⁷ Arguments presented in [20] show, however, that it is at least possible for domain walls of purely QCD origin to live for macroscopically large lifetimes.

To summarize, we have a QCD domain wall with all of the properties required to generate magnetic fields:

1. The walls form shortly after the QCD phase transition and attain Hubble-scale correlations through the Kibble mechanism.
2. The QCD domain walls have a structure on the scale of $m_{\eta'}^{-1} \sim \Lambda_{\text{QCD}}^{-1}$ and thus they can efficiently interact with nucleons and other QCD matter.
3. The transition in the singlet η' field produces an environment near the wall where the effective θ parameter is non-zero. Thus, across the wall, there is maximal CP violation. In such an environment, it is known that the electric and magnetic dipole moments of the nucleons are of the same order [21].
4. The strong CP violation also provides a mechanism for generating helicity on a Hubble scale⁸ by aligning both the electric and magnetic dipole moments along the domain wall.
5. The decay mechanism described in [20] renders the QCD domain walls unstable such that the walls themselves do not pose a cosmological problem. However, the suppression in the decay mechanism due to quantum tunneling might extend the lifetime of the walls to a macroscopic scale (22) which is long enough to generate the required electromagnetic turbulence as we shall show.

⁷ It is possible to regain control of the calculation in the high density limit. See the discussion in section (VIII A).

⁸ To be precise, the domain walls separate the helicity into Hubble size regions to that globally the total helicity is zero, but within Hubble scale regions, the helicity is maximal and correlated with the same sign.

VI. ALIGNMENT OF SPINS IN THE DOMAIN WALL

Now we shall show that the domain walls indeed do acquire a magnetization and present a simplified method for estimating the magnitudes of bulk properties on the domain wall. This method makes the approximation that the domain wall is flat and that translational and rotational symmetries are preserved in the plane of the wall (which we take to be the x - y plane.) These approximations are valid in the case of domain walls whose curvature is large in comparison to the length scale of the pertinent physics.

Once this approximation is made, we can reformulate the problem in 1 + 1 dimensions (z and t) and calculate the density of the desired bulk properties along the domain wall. To regain the full four-dimensional bulk properties, we must estimate the density of the particles in the x - y plane to obtain the appropriate density and degeneracy factors for the bulk density. Thus, the final results are not independent of physics in the x - y plane, but rather, these effects are accounted for only through the degeneracy factors.

We proceed to demonstrate this technique by calculating the alignment of fermionic spins along the wall. We take the standard form for the interaction between the pseudo-scalar η' field and the nucleons which respects all relevant symmetries:

$$\mathcal{L}_4 = \bar{\Psi} (i\not{\partial} - m_N e^{i\phi\gamma_5}) \Psi. \quad (23)$$

Here $\phi = \phi(z)$ characterizes our domain wall solution as expressed in Equation (15) and m_N is the nucleon mass. For our approximations, we assume that fluctuations in the nucleon field Ψ do not affect the domain walls and, thus, treat the domain walls as a background field⁹. The strategy is to break (23) into two 1 + 1 dimensional components by setting $\partial_x = \partial_y = 0$ (this is the approximation that the physics in the z direction decouples from the physics in the x - y plane) and then by manipulating the system of equations that result.

First, we introduce the following chiral components of

the Dirac spinors¹⁰:

$$\Psi_+ = \frac{1}{\sqrt{S}} \begin{pmatrix} \chi_1 \\ \chi_2 \end{pmatrix}, \quad \Psi_- = \frac{1}{\sqrt{S}} \begin{pmatrix} \xi_1 \\ \xi_2 \end{pmatrix}, \quad (24)$$

$$\Psi = \frac{1}{\sqrt{2S}} \begin{pmatrix} \chi_1 + \xi_1 \\ \chi_2 + \xi_2 \\ \chi_1 - \xi_1 \\ \chi_2 - \xi_2 \end{pmatrix} = \frac{1}{\sqrt{2}} \begin{pmatrix} \Psi_+ + \Psi_- \\ \Psi_+ - \Psi_- \end{pmatrix}, \quad (25)$$

where S is the area of the wall. This normalization factor cancels the degeneracy factor proportional to S added in the next subsection. Now we re-express (23) by noting that $\gamma_5^2 = I$:

$$\mathcal{L}_4 = \bar{\Psi} \left[i \begin{pmatrix} \partial_0 & -\sigma_j \partial_j \\ \sigma_j \partial_j & -\partial_0 \end{pmatrix} - m_N \begin{pmatrix} \cos(\phi) & i \sin(\phi) \\ i \sin(\phi) & \cos(\phi) \end{pmatrix} \right] \Psi.$$

The associated Dirac equation is

$$\left[i \begin{pmatrix} \partial_0 & -\sigma_j \partial_j \\ \sigma_j \partial_j & -\partial_0 \end{pmatrix} - m_N \begin{pmatrix} \cos(\phi) & i \sin(\phi) \\ i \sin(\phi) & \cos(\phi) \end{pmatrix} \right] \Psi = 0.$$

This is equivalent to the coupled system:

$$2i(\partial_0 + \sigma_i \partial_i) \Psi_- = 2m_N e^{i\phi} \Psi_+, \quad (26a)$$

$$2i(\partial_0 - \sigma_i \partial_i) \Psi_+ = 2m_N e^{-i\phi} \Psi_-. \quad (26b)$$

Now, we decouple the z coordinates from x and y by setting $\partial_x = \partial_y = 0$:

$$i \begin{pmatrix} \partial_t + \partial_z & 0 \\ 0 & \partial_t - \partial_z \end{pmatrix} \Psi_- = m_N e^{i\phi} \Psi_+, \quad (27a)$$

$$i \begin{pmatrix} \partial_t - \partial_z & 0 \\ 0 & \partial_t + \partial_z \end{pmatrix} \Psi_+ = m_N e^{-i\phi} \Psi_-. \quad (27b)$$

Both these equations are diagonal. Thus, we see that the top components and bottom components of Ψ_{\pm} mix independently.

$$\begin{pmatrix} -m_N e^{i\phi} & i(\partial_t + \partial_z) \\ i(\partial_t - \partial_z) & -m_N e^{-i\phi} \end{pmatrix} \begin{pmatrix} \chi_1 \\ \xi_1 \end{pmatrix} = 0, \quad (28a)$$

$$\begin{pmatrix} -m_N e^{i\phi} & i(\partial_t - \partial_z) \\ i(\partial_t + \partial_z) & -m_N e^{-i\phi} \end{pmatrix} \begin{pmatrix} \chi_2 \\ \xi_2 \end{pmatrix} = 0. \quad (28b)$$

Remember that we are looking for a two-dimensional Dirac equation, thus we want the kinetic terms to look

⁹ A full account would take into account the effects of this back-reaction. We expect that such back-reactions would affect the potential (9) by altering the form of the last term and possibly adding higher order corrections. This may affect the magnitudes of some of the estimates, but would certainly not alter the topology of the fields and thus the domain walls would still form with a similar structure. Quantitatively this would alter the results, but not the order of magnitude.

¹⁰ We are using the standard representation here:

$$\gamma_0 = \begin{pmatrix} I & 0 \\ 0 & -I \end{pmatrix}, \quad \gamma_j = \begin{pmatrix} 0 & \sigma_j \\ -\sigma_j & 0 \end{pmatrix}, \quad \gamma_5 = \begin{pmatrix} 0 & I \\ I & 0 \end{pmatrix},$$

$$\sigma_1 = \begin{pmatrix} 0 & 1 \\ 1 & 0 \end{pmatrix}, \quad \sigma_2 = \begin{pmatrix} 0 & -i \\ i & 0 \end{pmatrix}, \quad \sigma_3 = \begin{pmatrix} 1 & 0 \\ 0 & -1 \end{pmatrix}.$$

the same. For this reason we should flip the rows and columns of the second equation. Doing this and defining the two two-dimensional spinors

$$\Psi_{(1)} = \begin{pmatrix} \chi_1 \\ \xi_1 \end{pmatrix}, \quad \Psi_{(2)} = \begin{pmatrix} \xi_2 \\ \chi_2 \end{pmatrix}, \quad (29)$$

the equations have the following structure:

$$(i\hat{\gamma}^\mu \partial_\mu - m_N e^{+i\phi\hat{\gamma}_5})\Psi_{(1)} = 0 \quad (30a)$$

$$(i\hat{\gamma}^\mu \partial_\mu - m_N e^{-i\phi\hat{\gamma}_5})\Psi_{(2)} = 0 \quad (30b)$$

where the index $\mu \in \{t, z\}$, the Lorentz signature is $(1, -1)$ and we define the following two-dimensional version of the gamma matrices:

$$\hat{\gamma}_t = \sigma_1, \quad \hat{\gamma}_z = -i\sigma_2, \quad \hat{\gamma}_5 = \sigma_3.$$

These satisfy the proper two-dimensional relationships $\hat{\gamma}_5 = \hat{\gamma}_t \hat{\gamma}_z$ and $\hat{\gamma}_\mu \hat{\gamma}_\nu = g_{\mu\nu} + \epsilon_{\mu\nu} \hat{\gamma}_5$. We can reproduce equation (30) from the following effective two-dimensional Lagrangian density,

$$\begin{aligned} \mathcal{L}_2 = & \bar{\Psi}_{(1)} (i\hat{\gamma}^\mu \partial_\mu - m_N e^{+i\phi\hat{\gamma}_5}) \Psi_{(1)} + \\ & + \bar{\Psi}_{(2)} (i\hat{\gamma}^\mu \partial_\mu - m_N e^{-i\phi\hat{\gamma}_5}) \Psi_{(2)}, \end{aligned} \quad (31)$$

where two different species of fermion with opposite chiral charge interact with the domain wall background $\phi(z)$. Note that, due to the normalization factor $1/\sqrt{S}$ we introduced above, the two-dimensional fields $\Psi_{(i)}$ have the correct canonical dimension $1/2$.

We have thus successfully reduced our problem to a two-dimensional fermionic system. It is known that for several systems in $1+1$ dimensions, the fermionic representation is equivalent to a $1+1$ dimensional bosonic system through the following equivalences¹¹ [54, 55]:

$$\bar{\Psi}_{(j)} i\hat{\gamma}^\mu \partial_\mu \Psi_{(j)} \rightarrow \frac{1}{2} (\partial_\mu \theta_j)^2, \quad (32a)$$

$$\bar{\Psi}_{(j)} \hat{\gamma}_\mu \Psi_{(j)} \rightarrow \frac{1}{\sqrt{\pi}} \epsilon_{\mu\nu} \partial^\nu \theta_j, \quad (32b)$$

$$\bar{\Psi}_{(j)} \Psi_{(j)} \rightarrow -\mu \cos(2\sqrt{\pi}\theta_j), \quad (32c)$$

$$\bar{\Psi}_{(j)} i\hat{\gamma}_5 \Psi_{(j)} \rightarrow -\mu \sin(2\sqrt{\pi}\theta_j). \quad (32d)$$

After making these replacements, we are left with the following two-dimensional bosonic effective Lagrangian density describing the two fields θ_1 and θ_2 in the domain wall background $\phi(z)$

$$\mathcal{L} = \frac{1}{2} (\partial_\mu \theta_1)^2 + \frac{1}{2} (\partial_\mu \theta_2)^2 - U(\theta_1, \theta_2) \quad (33)$$

¹¹ The constant μ in the last two equations is a scale parameter of order m_N . The exact coefficient of this term depends on the model and is only known for exactly solvable systems but in all cases, is of order unity. This technique is well-known to the condensed matter and particles physics communities. See for example [52, 53].

where the effective potential is

$$U(\theta_1, \theta_2) = -m_N \mu [\cos(2\sqrt{\pi}\theta_1 - \phi) + \cos(2\sqrt{\pi}\theta_2 + \phi)]. \quad (34)$$

The next approximation that we make is to neglect the dynamics of the θ_k fields: we assume that they relax slowly in the domain wall background such that their dynamics do not contribute appreciably to the final state¹² which minimizes the potential (34). The classical minimizing solution is thus

$$\langle \theta_1 \rangle = \frac{\phi}{2\sqrt{\pi}}, \quad \langle \theta_2 \rangle = \frac{-\phi}{2\sqrt{\pi}}. \quad (35)$$

We are now ready to show that the domain walls align the spins of the fermions. The relevant spin operator is¹³

$$\Psi^\dagger \vec{\Sigma} \Psi = \bar{\Psi} \vec{\gamma} \gamma_5 \Psi = \Psi_+^\dagger \vec{\sigma} \Psi_+ + \Psi_-^\dagger \vec{\sigma} \Psi_- \quad (36)$$

Let us consider the z component of the spin. We then have

$$\begin{aligned} \Psi^\dagger \Sigma_z \Psi &= \frac{1}{S} (\chi_1^\dagger \chi_1 - \chi_2^\dagger \chi_2 + \xi_1^\dagger \xi_1 - \xi_2^\dagger \xi_2) \\ &= \frac{1}{S} (\bar{\Psi}_{(1)} \hat{\gamma}_t \Psi_{(1)} - \bar{\Psi}_{(2)} \hat{\gamma}_t \Psi_{(2)}) \end{aligned} \quad (37)$$

and so we see that the four-dimensional spin operator $\Sigma_z = \gamma_0 \gamma_z \gamma_5$ is expressed in terms of a pair of two-dimensional fermion charge operators. We can calculate the expectation value of the spin operator in the domain wall background using this two-dimensional correspondence (37) and the bosonic representation of the fermions

$$\begin{aligned} \Psi^\dagger \Sigma_z \Psi &= \frac{1}{S} (\bar{\Psi}_{(1)} \hat{\gamma}_t \Psi_{(1)} - \bar{\Psi}_{(2)} \hat{\gamma}_t \Psi_{(2)}) \\ &= \frac{1}{S\sqrt{\pi}} \partial_z (\theta_2 - \theta_1). \end{aligned} \quad (38)$$

Finally, we use our minimizing bosonic solution (35) to obtain the following four-dimensional average spin aligned along the domain wall:

$$\langle \Psi^\dagger \Sigma_z \Psi \rangle = -\frac{1}{S\pi} \frac{\partial \phi(z)}{\partial z}. \quad (39)$$

We will also need the following matrix elements later on:

$$\begin{aligned} \langle \bar{\Psi} i\sigma_{xy} \Psi \rangle &= \langle \bar{\Psi} \sigma_{tz} \gamma_5 \Psi \rangle = \left\langle \Psi^\dagger \begin{pmatrix} \sigma_3 & 0 \\ 0 & -\sigma_3 \end{pmatrix} \Psi \right\rangle \\ &= \frac{1}{S} (\chi_1^\dagger \xi_1 - \chi_2^\dagger \xi_2 + \xi_1^\dagger \chi_1 - \xi_2^\dagger \chi_2) \\ &= \frac{1}{S} \langle \bar{\Psi}_{(1)} \Psi_{(1)} \rangle - \frac{1}{S} \langle \bar{\Psi}_{(2)} \Psi_{(2)} \rangle \\ &= 0 \end{aligned} \quad (40)$$

¹² This is the same adiabatic approximation used by Goldstone and Wilczek [52].

¹³ Here we use the convention that $\sigma_{ij} = \frac{1}{2} [\gamma_i, \gamma_j]$, thus the spin operator $\Sigma_k \equiv \frac{i}{2} \epsilon_{ijk} \sigma_{ij}$. In matrix form with the standard representation, this becomes:

$$\Sigma_k = \epsilon_{ijk} \frac{i}{4} \begin{pmatrix} -[\sigma_i, \sigma_j] & 0 \\ 0 & -[\sigma_i, \sigma_j] \end{pmatrix} = \begin{pmatrix} \sigma_k & 0 \\ 0 & \sigma_k \end{pmatrix}.$$

In terms of the gamma matrices, this is $\Sigma_k = \gamma_0 \gamma_k \gamma_5$.

and

$$\begin{aligned}
-\langle \bar{\Psi} i \sigma_{tz} \Psi \rangle &= \langle \bar{\Psi} \sigma_{xy} \gamma_5 \Psi \rangle = \left\langle \Psi^\dagger \begin{pmatrix} 0 & -i\sigma_3 \\ i\sigma_3 & 0 \end{pmatrix} \Psi \right\rangle \\
&= \frac{i}{S} \langle -\xi_1^\dagger \chi_1 + \xi_2^\dagger \chi_2 + \chi_1^\dagger \xi_1 - \chi_2^\dagger \xi_2 \rangle \\
&= -\frac{1}{S} \langle \bar{\Psi}_{(1)} i \gamma_5 \Psi_{(1)} \rangle + \frac{1}{S} \langle \bar{\Psi}_{(2)} i \gamma_5 \Psi_{(2)} \rangle \\
&= \frac{2\mu}{S} \sin(\phi) \tag{41}
\end{aligned}$$

Remember that we have restricted ourselves to a 1 + 1 dimensional theory. We must now estimate the density and degeneracy of the nucleons along the wall so we can obtain a true 1 + 3 dimensional estimate of the spin density.

A. Fermion Degeneracy in the Domain Wall

We have assumed that locally the domain walls have only a spatial z dependence. There is still a two-dimensional translational and rotational symmetry in the x - y plane. These translational degrees of freedom imply that momentum in the plane is conserved and hence we can treat the neglected degrees of freedom for the fermions as free. The degeneracy in a region of area S will simply be a sum over these degrees of freedom with a discrete factor $g = 4 = 2 \times 2$ for spin and isospin degeneracy

$$N = g \int_{\substack{\vec{x} \in S \\ \|\vec{p}\| < p_F}} dx dy \frac{dp_x}{2\pi} \frac{dp_y}{2\pi} = g \frac{S \pi p_F^2}{4\pi^2} \sim g \frac{S \Lambda_{\text{QCD}}^2}{4\pi}. \tag{42}$$

Here we estimate the Fermi momentum $p_F \approx \Lambda_{\text{QCD}}$ by the thermal scale of the fermions¹⁴ and assume that the Fermi sea is filled¹⁵.

This completes our estimate of the induced spin along the domain wall in a small region S . Combining our estimate of the spin (39) from the bosonization scheme with the fermion degeneracy (42) we obtain the spin density along the wall:

$$\langle \Psi^\dagger \Sigma_z \Psi \rangle_{4D} = \frac{\Lambda_{\text{QCD}}^2}{\pi^2} \frac{\partial \phi(z)}{\partial z}. \tag{43}$$

As a check, note that, the dimension here is 3 and, the result does not depend on the normalization factor S .

¹⁴ We are treating the fermions along the wall as a massless, two-dimensional Fermi-gas.

¹⁵ Voloshin obtained a similar estimate [23]. Furthermore, he estimates that there are sufficiently many fermions in the Hubble volume to diffuse into the domain wall potential justifying our assumption about the filled Fermi sea.

VII. GENERATION OF ELECTROMAGNETIC FIELD

Once the spins are aligned, the nucleon electric and dipole moments interact with the electromagnetic fields $F_{\mu\nu}$ through the interaction

$$\frac{1}{2} (d_\Psi \bar{\Psi} \sigma_{\mu\nu} \gamma_5 \Psi + \mu_\Psi \bar{\Psi} i \sigma_{\mu\nu} \Psi) F^{\mu\nu} + \bar{\Psi} (i D_\mu) (i D^\mu) \Psi. \tag{44}$$

Here the nucleons have both electric and magnetic dipole moments $d_\Psi \sim \mu_\Psi$ respectively (5).

Now, we make the approximation again that the nucleons align independently of the electromagnetic field, and we treat the nucleon field Ψ as a background. The situation is a field of dipoles aligned along the domain wall. The net fields generated by surface of area ξ^2 willed with a constant density of aligned dipoles is proportional to ξ^{-1} since the dipoles tend to cancel. For a perfectly flat domain wall of infinite extent, $\xi \rightarrow \infty$ and thus no net field would remain as pointed out in [23]. The QCD domain walls, however, are far from flat: the walls have many wiggles and high frequency dynamics excitations. Thus, the fields generated by the dipoles will not cancel on the domain wall, but will be suppressed by a factor¹⁶ of $(\xi \Lambda_{\text{QCD}})^{-1}$ where ξ is an effective correlation length that depends on the dynamics of the domain walls. As an upper bound, the extent of the domain walls is limited by the Hubble scale. Typically, domain walls remain space filling, thus we expect $\Lambda_{\text{QCD}}^{-1} \leq \xi \ll \text{Hubble scale}$. Unfortunately, we presently cannot make a tighter bound on ξ , however, we shall see that, even in the worst case, this mechanism can at least generate feasible seed fields for galactic dynamos to amplify.

The result of sections (VI) and (VIA) is a method for estimating the strengths of various sources in the domain walls. We now need to couple these to the generation of electromagnetic turbulence. To do this properly requires the solution to Maxwell's equations as coupled to the sources in (44). This is difficult, though no doubt important for accurate numerical estimates, and so for an order of magnitude estimate we consider a dimensional estimate considering the sources as a set of dipoles sitting in the domain walls. The spacing between the dipoles is set by the QCD scale $\Lambda_{\text{QCD}}^{-1}$, and the strengths of the field can be estimated from (44) using dimensional arguments:

$$\langle F_{\mu\nu} \rangle \sim \frac{1}{\xi \Lambda_{\text{QCD}}} (d_\Psi \langle \bar{\Psi} \sigma_{\mu\nu} \gamma_5 \Psi \rangle + \mu_\Psi \langle \bar{\Psi} i \sigma_{\mu\nu} \Psi \rangle). \tag{45}$$

This includes the dipole suppression discussed above. From (40), (41), (42) and (45) we arrive at the following estimates for the average electric and magnetic fields

¹⁶ The density of the dipoles is governed by the QCD scale $\Lambda_{\text{QCD}}^{-1}$.

(correlated on the Hubble scale) which includes the degeneracy factors (remember that $\mu \approx m_N$):

$$|\langle E_z \rangle| \sim |\langle B_z \rangle| \sim \frac{0.5 e \Lambda_{\text{QCD}}^2}{\pi \xi \Lambda_{\text{QCD}}} \sim \frac{10^{17} \text{ G}}{\xi \Lambda_{\text{QCD}}} \quad (46)$$

This method of estimating the electric and magnetic fields produced is extremely crude: we have not solved Maxwell's equations, we have not taken back reactions into account and we have not fully accounted for the motion and geometry of the domain walls. Never the less, we expect that the estimates (46) to be valid as an order of magnitude estimate for the field strengths. The approximations we have made and effects that we have neglected will be discussed in section (VIII A). Thus, we have the approximations for the fields (46) which, along with (2), justifies the estimate (1).

A. Helicity

Finally, we note that the turbulence discussed in section (III) should be highly helical. This helicity arises from the fact that both electric and magnetic fields are correlated together along the entire domain wall, $\langle \vec{E} \rangle \sim \langle \vec{A} \rangle / \tau$ where $\langle \vec{A} \rangle$ is the vector potential and τ is a relevant timescale for the electrical field to be screened (we expect $\tau \sim \Lambda_{\text{QCD}}^{-1}$ as we discuss below). The magnetic helicity density is thus:

$$h \sim \vec{A} \cdot \vec{B} \sim \tau \langle E_z \rangle \langle B_z \rangle \sim \tau \frac{e^2 \Lambda_{\text{QCD}}^2}{\pi^2 \xi^2}. \quad (47)$$

It can be seen from (45) that both the electric field and magnetic fields have the same structure in the domain wall. This implies that domain walls (solitons) have the same sign of helicity everywhere. Under CP the wall becomes an “anti-wall” (anti-soliton) and the orientation of the magnetic field B changes direction: thus anti-walls have opposite helicity.

Note carefully what happens here: The total helicity was zero in the quark-gluon-plasma phase and remains zero in the whole universe, but the helicity is separated so that in one Hubble volume where one domain wall dominates, the helicity has the same sign. The reason for this is that, as the domain walls coalesce, initial perturbations cause either a soliton or an anti-soliton to dominate and fill the Hubble volume. In the neighboring space, there will be other solitons and anti-solitons so that there is an equal number of both, but they are separated and this spatial separation prevents them from annihilating. This is similar to how a particle and anti-particle may be created and then separated so they do not annihilate. In any case, the helicity is a pseudo-scalar and thus maintains a constant sign everywhere along the domain wall: thus, the entire Hubble volume is filled with helicity of the same sign. This is the origin of the Hubble scale correlations in the helicity and in B^2 . The correlation parameter ξ

which affects the magnitude of the fields plays no role in disturbing this correlation.

As we mentioned, eventually, the electric field will be screened. The timescale for this is set by the plasma frequency for the electrons (protons will screen much more slowly) ω_p which turns out to be numerically close to Λ_{QCD} near the QCD phase transition. The nucleons, however, also align on a similar timescale $\Lambda_{\text{QCD}}^{-1}$, and the helicity is generated on this scale too, so the electric screening will not qualitatively affect the mechanism.¹⁷ Finally, we note that the turbulence requires a seed which remains in a local region for a timescale set by the conductivity [56] $\sigma \sim cT/e^2 \sim \Lambda_{\text{QCD}}$ where for $T = 100$ MeV, $c \approx 0.07$ and is smaller for higher T . Thus, even if the domain walls move at close to the speed of light (due to vibrations), there is still enough time to generate turbulence throughout the Hubble volume.

VIII. CONCLUSION

A. Summary

Here is a brief summary of what we have done and the approximations that were made:

1) In section (IV B) we outlined the generic features that domain wall models should possess if they are to successfully generate primordial seeds by the method described in this paper. We proceeded with the QCD domain wall model [20] to estimate the magnitude of the effects¹⁸.

2) Making the approximation of thin flat domain walls we proceeded to calculate the averages of quantities like $\langle \bar{\Psi} i \sigma_{\mu\nu} \Psi \rangle$ by reducing the interaction (23) to a 1 + 1 dimensional system. In this approximation we discarded the momenta in the x - y plane to get (27). We capture the effects of these momenta by degeneracy factors in

¹⁷ If the screening were more efficient, then one might worry that the electric field would not last long enough to generate the helicity.

¹⁸ Further support for the existence of QCD domain walls comes from calculations presented in [57] where it is shown that these walls almost certainly exist in the high density regime of QCD. Thus, domain walls seem to be important features at high density. Furthermore, if one accepts a conjecture on quark-hadron continuity at low temperature with respect to variations in the chemical potential μ [58], then one can make the following argument: If for large μ domain walls exist, but for low μ they do not, then there should be some sort of phase transition as one lowers μ . Thus, the continuity conjecture supports the existence of quasi-stable QCD domain walls at lower densities, at least down to the densities of hyper-nuclear matter. Coupled with the fact that gluon and quark condensates do not vary much as one moves from the domain of hyper-nuclear matter to the low density limit, one suspects that the qualitative picture holds even for zero density. Different arguments based on large N_c counting, also support the existence of the meta-stable QCD domain walls at zero chemical potential μ [20].

section (VIA). This approximation is valid only if the physics in the z direction is independent of motion in the x - y plane. This approximation breaks down when thermal (or other) fluctuations are large enough that the physics in the z - t directions no longer decouple from the physics in the x - y plane.

In making estimates like (39), another approximation we have made is to ignore back reactions. We have treated the domain wall as a static background: in reality, the presence of fermions in the domain wall would affect the structure. What we say is that such back reactions will not change the overall structure or scale of the phenomenon, however, it will definitely alter the quantitative results. Thus, estimates like (39) should only be taken as qualitative approximations to the structure in the domain wall. A comprehensive analysis would take into account the effects of fermions on the domain walls through additional interactions to (8). These interactions, however, would not alter the $U(1)$ nature of the η' field, and thus the basic domain wall structure would still be present. Also, it is unlikely that the back-reaction of the electromagnetic fields can substantially affect the domain wall structure or the alignment of the spins. Indeed, the domain walls and the spin alignment are due to QCD interactions on the scale Λ_{QCD} . Any back-reaction, would be suppressed at least by a factor of $\alpha \sim 1/137$, thus, the quantitative results might be altered, but we expect the qualitative behaviour and orders of magnitudes to be preserved.

3) The next step was to estimate the strengths of the generated fields by using dimensional arguments and considering a collection of dipoles aligned in the domain wall background arriving at the estimates (46). The actual fields generated will be sensitive to the geometry and dynamics of the domain walls: this is something that we need to understand much better. We have captured these effects in the unknown scale length ξ but there is much we could understand about this. To study these effects we will need to solve Maxwell's equations (44), however, in the non-trivial geometry of the domain walls we will probably have to simulate this. Of particular importance is the question: Can the larger fields be generated by the motion of the domain walls?

The interaction of the fields with the plasma is also important, as the electric fields may be screened. Simple estimates, however, show that the screening timescale is at least as long as the other timescales.

4) We have estimated the scaling of the magnetic turbulence (2) and showed that the fields generated by domain walls at the QCD phase transition would be of astrophysical interest. The point we make here is that fields are generated and correlated on the same length as the domain walls. Thus, the domain walls provide a mechanism for generating Hubble scale correlations.

Without a better understanding of the dynamics of the domain walls, we cannot better estimate the field strengths, but it is possible that the generated fields are quite large (nanogauss to microgauss scale) even

without any amplification. It seems that the fields will still require some amplification by galactic dynamos, but these primordial seeds provide the large scale correlation lengths that have been difficult to achieve through other mechanisms.

We have seen that domain walls at the QCD phase transition may provide a nice way to resolve some of the problems with generating large scale magnetic fields. It is important to note that the mechanism described here is seated in well-established physics and makes definite predictions. The only free ‘‘parameter’’ is a correlation length ξ which affects only the strengths of the fields generated. This parameter is not really free, but represents our lack of understanding of the formation and dynamics domain walls. As this understanding is improved, the scale of this parameter will be fixed, and the method will make a definite prediction about the strengths of the fields.

Thus, this mechanism is testable: it already makes a definite prediction about the order of the field correlation lengths: If fields are observed to have much large correlations that 500 kpc, then either a more efficient inverse cascade mechanism must be discovered or another method (possibly inflationary) must be considered to generate these correlation lengths.

B. Speculations and Future Directions

This mechanism has been a first attempt to describe astrophysical consequences of recently conjectured QCD domain walls [20]. These walls may affect several areas of astrophysics, both through the field generation mechanism described here and through other effects. We discuss several of these applications below.

The most promising possibility to test the idea of primordial seeds is to measure extra-galactic and extra-cluster magnetic fields. This may be possible in the near future through measurements of anisotropies in the cosmic microwave background (CMB) radiation spectrum [59, 60] or through non-thermal radiation from Compton scattering of relativistic electrons off of the CMB [61]. Current CMB observations [62] place upper bounds on the strengths of primordial fields, which the fields described in this paper respect. There are other limits imposed on the strengths of primordial magnetic fields from nucleosynthesis production rates, all of which this mechanism respect. For a thorough review, see [5].

There are many possible consequences of primordial magnetic fields discussed in [5], but we point out a particularly interesting possibility that might support domain wall generated fields. It seems that certain types of field structures might explain the apparent violations of the GZK cutoff [63]. It is likely that primordial fields from domain walls may possess a planar structure that could assist in explaining these violations.

Independent of the magnetic fields, QCD domain walls might affect early cosmology in another way. As we dis-

cussed in the text, baryons are concentrated on the wall causing inhomogeneities in the baryon density. While it seems that QCD domain walls will decay before $T = 1$ MeV, the inhomogeneity in baryon density must be redistributed by diffusion and other dissipative processes and thus inhomogeneities might persist that affect nucleosynthesis.

Recent measurements of the CMB by BOOMERANG [64] and MAXIMA [65] lead to a value of baryon density Ω_B is larger than the value allowed by the conventional model. The agreement can be achieved [66] through inhomogeneous big bang nucleosynthesis (IBBN) if regions of baryon inhomogeneity are separated by a distance scale of about 70 km (at $T = 1$ MeV), and if these regions have a planar structure with high surface to volume ratio. Models have been proposed whereby such a planar structure can occur [67], however, we suggest that QCD domain walls might automatically create this kind of structure with the appropriate scale if the baryon diffusion and other dissipative processes are sufficiently slow (or if something extends the lifetime of the QCD domain walls beyond the estimate (22)). Conversely, nucleosynthesis provides another constraint to check the validity of QCD domain wall properties. Additional work is required [68] before any definite statements can be made.

At this point, we would like to comment on a speculative application of QCD domain walls that may be of significant astrophysical interest. Given that QCD domain walls are very stable at high densities [57], it is not inconceivable that the accumulation of baryons along the domain wall by a mechanism similar to that described in section (VI) may stabilize the the domain walls so that they survive much longer than (22). If this is the case, then QCD domain walls might form the seeds for primordial baryonic compact objects. Such objects would certainly affect nucleosynthesis, the cosmic microwave background radiation spectrum and possible structure formation. The result, however, would be stable, cold, “invisible” baryonic matter that would contribute to the dark matter. In addition, this matter would have QCD scale cross-section recently suggested for dark matter [69] to explain several discrepancies with the standard cold dark matter picture. Besides that, this matter would offer a simple explanation of why observations find $\Omega_{Dark} \sim \Omega_B$ to within an order of magnitude. This fact is extremely

difficult to explain in models where a dark matter candidate is related to a physics independent of baryogenesis. Without further calculations, it is not possible to make even qualitative predictions about these speculations, but, as our understanding improves, such a model would be able to make definite predictions. Furthermore, the physics of QCD domain walls may lend itself to signatures that can be tested in relativistic heavy ion collisions. This might provide some concrete foundations for QCD phenomena affecting cosmology and astrophysics. Likewise, the accuracy of nuclear abundance measurements and CMB anisotropy measurements could provide serious constraints on the behaviour of QCD phenomena related to domain walls. Thus, while we cannot yet seriously advocate the idea of compact primordial baryonic objects forming from this mechanism, one should at least keep them in mind when studying these and similar processes.

We would like to close by emphasizing the relationship that is developing between astrophysics and particle physics at the QCD scale. Particle physics provides concrete models for astrophysical phenomena that, as our understanding of fundamental physics increases, has definite predictive power. Thus, there is the potential to ground many astrophysical phenomena in well founded, testable physics. In return, astrophysical observations provide a means for testing particle physics theories under conditions not possible on earth. We eagerly await the fruitful developments that will result from this reciprocal relationship.

Acknowledgments

This work was supported by the NSERC of Canada. We would like to thank R. Brandenberger for many useful discussions. AZ wishes to thank: P.Steinhardt and M. Turner for valuable discussions; L. McLerran and D. Son for discussions on Silk damping; and M. Voloshin and A. Vainshtein for discussions on the magnetic properties of domain walls. MF wishes to thank F. Wilczek and K. Rajagopal for useful discussions about high density matter and astrophysics.

-
- [1] M. M. Forbes and A. R. Zhitnitsky, Phys. Rev. Lett. **85**, 5268 (2000), hep-ph/0004051.
 - [2] M. M. Forbes and A. R. Zhitnitsky, (2000), hep-ph/0008318.
 - [3] P. P. Kronberg, Rept. Prog. Phys. **57**, 325 (1994).
 - [4] R. Beck, A. Brandenburg, D. Moss, A. Shukurov, and D. Sokoloff, Ann. Rev. Astron. Astrophys. **34**, 155 (1996), NORDITA-95-67-A.
 - [5] D. Grasso and H. R. Rubinstein, (2000), astro-ph/0009061.
 - [6] O. Tornkvist, (2000), astro-ph/0004098.
 - [7] P. Olesen, (1997), hep-ph/9708320.
 - [8] M. S. Turner and L. M. Widrow, Phys. Rev. **D37**, 2743 (1988).
 - [9] T. Vachaspati and A. Vilenkin, Phys. Rev. Lett. **67**, 1057 (1991).
 - [10] M. Gasperini, M. Giovannini, and G. Veneziano, Phys. Rev. Lett. **75**, 3796 (1995), hep-th/9504083.
 - [11] A. Dolgov and J. Silk, Phys. Rev. **D47**, 3144 (1993).
 - [12] M. Joyce and M. E. Shaposhnikov, Phys. Rev. Lett. **79**,

- 1193 (1997), astro-ph/9703005.
- [13] G. Baym, D. Bodeker, and L. McLerran, Phys. Rev. **D53**, 662 (1996), hep-ph/9507429.
- [14] G. Sigl, A. V. Olinto, and K. Jedamzik, Phys. Rev. **D55**, 4582 (1997), astro-ph/9610201.
- [15] A. Brandenburg, K. Enqvist, and P. Olesen, Phys. Rev. **D54**, 1291 (1996), astro-ph/9602031.
- [16] P. Olesen, Phys. Lett. **B398**, 321 (1997), astro-ph/9610154.
- [17] A. Iwazaki, Phys. Rev. Lett. **79**, 2927 (1997), hep-ph/9705456.
- [18] P. Cea and L. Tedesco, Phys. Lett. **B425**, 345 (1998), hep-th/9711011;
P. Cea and L. Tedesco, Phys. Lett. **B450**, 61 (1999), hep-th/9811221.
- [19] A. Vilenkin and E. P. S. Shellard, *Cosmic Strings and Other Topological Defects*, paperback (2000) ed. (Cambridge University Press, Cambridge, 1994).
- [20] M. M. Forbes and A. R. Zhitnitsky, (2000), hep-ph/0008315.
- [21] R. J. Crewther, P. D. Vecchia, G. Veneziano, and E. Witten, Phys. Lett. **B88**, 123 (1979), **B91**, 487(E) (1980).
- [22] M. B. Voloshin, Phys. Lett. **B389**, 475 (1996), hep-ph/9609219.
- [23] M. B. Voloshin, (2000), hep-ph/0007123.
- [24] J. M. Cornwall, Phys. Rev. **D56**, 6146 (1997), hep-th/9704022.
- [25] D. T. Son, Phys. Rev. **D59**, 063008 (1999), hep-ph/9803412.
- [26] G. B. Field and S. M. Carroll, (1998), astro-ph/9811206.
- [27] A. Pouquet, U. Frisch, and J. Léorat, J. Fluid Mech. **77**, 321 (1976).
- [28] Y. B. Zeldovich, A. A. Ruzmaikin, and D. D. Sokoloff, *Magnetic Fields in Astrophysics* (McGraw Hill, New York, 1980).
- [29] A. R. Choudhuri, *The physics of fluids and plasmas: an introduction for astrophysicists* (Cambridge University Press, Cambridge, 1998).
- [30] K. Rajagopal and F. Wilczek, (2000), hep-ph/0011333.
- [31] M. C. Huang and P. Sikivie, Phys. Rev. **D32**, 1560 (1985).
- [32] S. Chang, C. Hagmann, and P. Sikivie, Phys. Rev. **D59** (1999), hep-ph/9807374.
- [33] G. Gabadadze and M. A. Shifman, Phys. Rev. **D62**, 114003 (2000), hep-ph/0007345.
- [34] R. D. Peccei and H. R. Quinn, Phys. Rev. Lett. **38**, 1440 (1977).
- [35] S. Weinberg, Phys. Rev. Lett. **40**, 223 (1978);
F. Wilczek, Phys. Rev. Lett. **40**, 279 (1978).
- [36] J. E. Kim, Phys. Rev. Lett. **43**, 103 (1979);
M. A. Shifman, A. I. Vainshtein, and V. I. Zakharov, Nucl. Phys. **B166**, 493 (1980).
- [37] M. Dine, W. Fischler, and M. Srednicki, Phys. Lett. **B104**, 199 (1981);
A. R. Zhitnitsky, Sov. J. Nucl. Phys. **31**, 260 (1980).
- [38] M. S. Turner, (1999), astro-ph/9912211.
- [39] H.-Y. Cheng, Phys. Rept. **158**, 1 (1988).
- [40] R. D. Peccei, Special topics: The strong CP problem, in *CP violation*, edited by C. Jarlskog, World Scientific, Singapore, 1989.
- [41] J. E. Kim, (1999), astro-ph/0002193.
- [42] I. Halperin and A. Zhitnitsky, Phys. Rev. Lett. **81**, 4071 (1998), hep-ph/9803301.
- [43] D. E. Groom *et al.*, Eur. Phys. J. **C15**, 1 (2000).
- [44] J. Gasser and H. Leutwyler, Phys. Rept. **87**, 77 (1982).
- [45] M. A. Shifman, A. I. Vainshtein, and V. I. Zakharov, Nucl. Phys. **B147**, 385 (1979).
- [46] E. Witten, Ann. Phys. **128**, 363 (1980).
- [47] P. D. Vecchia and G. Veneziano, Nucl. Phys. **B171**, 253 (1980).
- [48] A. Vilenkin and A. E. Everett, Phys. Rev. Lett. **48**, 1867 (1982).
- [49] P. Sikivie, Phys. Rev. Lett. **48**, 1156 (1982).
- [50] D. H. Lyth and E. D. Stewart, Phys. Rev. **D46**, 532 (1992).
- [51] T. W. B. Kibble, G. Lazarides, and Q. Shafi, Phys. Rev. **D26**, 435 (1982).
- [52] J. Goldstone and F. Wilczek, Phys. Rev. Lett. **47**, 986 (1981).
- [53] R. Jackiw and C. Rebbi, Phys. Rev. **D13**, 3398 (1976).
- [54] S. Mandelstam, Phys. Rev. **D11**, 3026 (1975).
- [55] S. Coleman, Phys. Rev. **D11**, 2088 (1975).
- [56] K. Dimopoulos and A.-C. Davis, Phys. Lett. **B390**, 87 (1997), astro-ph/9610013.
- [57] D. T. Son, M. A. Stephanov, and A. R. Zhitnitsky, (2000), hep-ph/0012041.
- [58] T. Schafer and F. Wilczek, Phys. Rev. Lett. **82**, 3956 (1999), hep-ph/9811473.
- [59] T. R. Seshadri and K. Subramanian, (2000), astro-ph/0012056.
- [60] T. Kahniashvili, A. Kosowsky, A. Mack, and R. Durrer, (2000), astro-ph/0011095.
- [61] Y. Rephaeli, (2000), astro-ph/0101363.
- [62] K. Jedamzik, V. Katalinic, and A. V. Olinto, Phys. Rev. Lett. **85**, 700 (2000), astro-ph/9911100.
- [63] G. R. Farrar and T. Piran, Phys. Rev. Lett. **84**, 3527 (2000), astro-ph/9906431.
- [64] A. E. Lange *et al.*, Phys. Rev. **D63**, 042001 (2001), astro-ph/0005004.
- [65] A. Balbi *et al.*, Astrophys. J. **545**, L1 (2000), astro-ph/0005124.
- [66] H. Kurki-Suonio and E. Sihvola, (2000), astro-ph/0011544.
- [67] B. Layek, S. Sanyal, and A. M. Srivastava, (2001), hep-ph/0101343.
- [68] M. M. Forbes and A. R. Zhitnitsky, In Preparation.
- [69] D. N. Spergel and P. J. Steinhardt, Phys. Rev. Lett. **84**, 3760 (2000), astro-ph/9909386.